An FT-EPR Investigation of the Anomalous CIDEP Observed in Photoinduced Reactions of Xanthone with Alcohols in the Presence of Hydrochloric Acid

Keishi Ohara[†] and Noboru Hirota*

Department of Chemistry, Graduate School of Science, Kyoto University, Kyoto 606, Japan

Debora M. Martino[‡] and Hans van Willigen*

Department of Chemistry, University of Massachusetts at Boston, Boston, Massachusetts 02125

Received: October 17, 1997; In Final Form: February 3, 1998

CIDEP spectra from free radicals produced by the photolysis of xanthone (Xn) in 2-propanol were investigated with FT-EPR. The spectra were assigned to the 2-hydroxypropan-2-yl (2HP) and xanthone ketyl (XnH) radicals. In pure 2-propanol and 2-propanol containing 10% H_2O, the spectra display low field emission/high field absorption with net emission (E*/A) type polarization. The observed CIDEP pattern is mainly due to the $S-T_0$ radical pair mechanism (RPM) with minor contributions from the triplet mechanism (TM) and radical triplet pair mechanism (RTPM). Upon addition of HCl, the polarization changes to net absorption. The rise time of the absorptive signals is determined by the response time of the spectrometer ($\sim 3 \times 10^{-8}$ s). Transient optical absorption measurements show that the triplet state of xanthone (^{3}Xn*) is quenched by HCl, and the change in spin polarization produced by HCl addition is attributed to this quenching process. The dependence of the CIDEP pattern and triplet xanthone lifetime on HCl concentration shows that both involve a diffusion-controlled process. The main ^{3}Xn* quenching process was found to be nonreactive, but it is proposed that its spin selectivity produces spin polarization in the products of the hydrogen abstraction reaction that runs in parallel with this quenching process.

Introduction

The spectroscopic and photochemical properties of xanthone (Xn) have been a topic of considerable interest in the past three decades.[1−17] It is well-known that the close proximity of the $^3\pi\pi^*$ and $^3n\pi^*$ states gives rise to unique features of triplet xanthone (^{3}Xn*). For example, the character of the lowest triplet state is strongly influenced by the solvent polarity,[2−6] and ^{3}Xn* shows the unusual phenomenon of dual phosphorescence.[1−3,5,6] Studies of photoexcited Xn have been performed with a variety of spectroscopic techniques such as transient absorption spectroscopy in the pico- and femtosecond time regions,[17] emission spectroscopy,[8,13,15] and magnetic resonance.[4,9−12]

In recent years, the time-resolved EPR (TREPR) technique has become a well-established method for investigating photochemical reactions and properties of photoexcited species. The phenomenon of chemically induced dynamic electron polarization (CIDEP) often provides valuable information not only on spin and reaction dynamics but also on precursor excited states.[18−20] For the most part, CIDEP producing mechanisms are now well understood.[21−28]

CIDEP studies have been made of a number of free radicals produced in photochemical reactions involving ^{3}Xn*. For instance, CW TREPR spectra have been reported of anion radicals produced by electron-transfer reactions from donors such as alkoxides,[10] ketyl radicals given by hydrogen abstraction reactions with phenols and alcohols,[14] and a cyclohexadienyl type radical by a hydrogen abstraction reaction with sodium borohydride.[11] Most of the CIDEP spectra obtained in these studies show net emissive or E*/A polarization (low field side emission and high field side absorption, the asterisk denoting excess net polarization). This polarization pattern can be accounted for in terms of a combination of two CIDEP mechanisms: (1) the triplet mechanism (TM), stemming from a sublevel-dependent intersystem crossing (isc) process in ^{3}Xn* which gives rise to emissive polarization; (2) the ST_0 radical pair mechanism (RPM) which is responsible for the E/A contribution to the polarization. This explanation is supported by the observation that ^{3}Xn* in a frozen matrix gives rise to a TREPR spectrum with emissive character.[12]

Recently, however, it was found that under certain conditions radicals produced in photochemical reactions of Xn could give rise to CW TREPR spectra exhibiting net absorptive polarization.[29] Photoreduction of Xn in alcohols by irradiation at 337 nm gives CIDEP spectra of the xanthone ketyl radical (XnH) and alcohol radicals with E/A* polarization. Moreover, upon addition of hydrochloric acid (HCl), spectra of these radicals become completely absorptive. It is noteworthy that benzophenone, which resembles Xn in structure and chemical properties, does not show this unusual change in CIDEP upon addition of HCl. Thus, the effect is a specific property of Xn. In the report by Koga et al.,[29] it was suggested that Xn forms a weak complex with HCl and that excitation of this complex might generate radicals that give rise to EPR spectra with absorptive polarization. However, it was found that HCl addition does not affect the emissive polarization pattern in the frozen solution CW TREPR spectrum of the Xn triplet, and there is no direct

* Corresponding authors.
[†] Present address: Department of Chemistry, Faculty of Science, Ehime University, Matsuyama 790-77, Japan.
[‡] On leave from the Physics Department, FBCB, UNL, 3000 Santa Fe, Argentina.

S1089-5639(97)03380-X CCC: $15.00
Published on Web 03/11/1998

spectroscopic evidence that ground-state complexes are formed. Therefore, further investigations are needed to clarify the mechanism by which HCl affects the spin polarization.

Fourier transform EPR (FT-EPR) offers both higher sensitivity and better spectral resolution than the CW TREPR technique. For these reasons, FT-EPR can provide new information about spin and reaction dynamics at the early stages of the photochemical reaction of Xn with alcohols. Since the time evolution measured by FT-EPR is free from microwave field perturbation, an analysis of the rise and decay of the EPR signals can reveal the intrinsic properties of the transient species more clearly. In the present work we have used FT-EPR to study the time development of transient EPR signals of 2-hydroxypropan-2-yl (2HP) and XnH radicals produced by photolysis of Xn in 2-propanol, a mixed solvent of 2-propanol and H_2O, and 2-propanol/H_2O with various amounts of HCl. In addition, optical absorption, emission, and transient absorption measurements were performed to complement the EPR data. Combining the results of the EPR and optical measurements, we show that dynamic quenching of ^{3}Xn* by HCl plays an important role and suggest a possible mechanism for the effect of this quenching process on spin polarization.

Experimental Section

FT-EPR measurements were performed at room temperature with a lab-built spectrometer described before.[30,31] A XeCl excimer laser (Lambda Physik EMG 103 MSC, 308 nm, 12 Hz repetition rate) was used for photoexcitation. Quadrature detected free induction decay (FID) signals were accumulated using the CYCLOPS phase-cycling procedure. The number of acquisitions per spectrum ranged from 400 to 1200. FT-EPR power spectra were obtained by Fourier transformation of the FID's. The time evolution of EPR signals was measured by changing the delay time between laser excitation and microwave pulse. The data acquisition and processing methods were the same as those reported previously.[31] The time resolution of the present experiments was estimated to be $\sim 3 \times 10^{-8}$ s; this value is mainly determined by the microwave and laser pulse widths and jitter in the timing of the pulses. Because the bandwidths of the spectra of the transient radicals far exceed the spectrometer bandwidth, complete spectra were assembled from FID's recorded with four to six field settings. The FT-EPR spectra shown here were converted to magnetic field representation (left side is low field, i.e., high frequency) for easy comparison with CW TREPR spectra.

CW TREPR measurements were carried out with a modified X-band EPR spectrometer (JEOL FE-3X).[32] CIDEP spectra were recorded with a boxcar integrator (PAR model 160). A XeCl excimer laser (Lumonics Hyper 400, 308 nm, 7.5 Hz) or a Nd:YAG laser (Quanta-Ray GCR-170, THG 355 nm, 10 Hz) was used for photoexcitation.

Transient absorption measurements were carried out with a lab-built spectrometer of conventional design[33] using a XeCl excimer laser for photoexcitation.

Xanthone and 2,6-di-*tert*-butylphenol (DTBP) were commercially available special grade reagents used without further purification. 2-Propanol and 2-methyl-1-propanol were G.R. grade reagents (Aldrich) used as received. Concentrated hydrochloric acid was used as received from EM Science (36.5% HCl, S.S.G.) in FT-EPR measurement or Wako Pure Chemical Industries (35%, S.S.G.) in the other measurements.

For FT-EPR measurements, the sample solutions were deoxygenated by purging with nitrogen gas before and during the experiments and pumped through a quartz cell held in the EPR cavity. The concentration of Xn was kept at 1.0×10^{-2} M, and the concentration of HCl ranged from 0 to 1.1 M. An addition of distilled water kept the water content in the samples containing HCl to 10% (v/v).

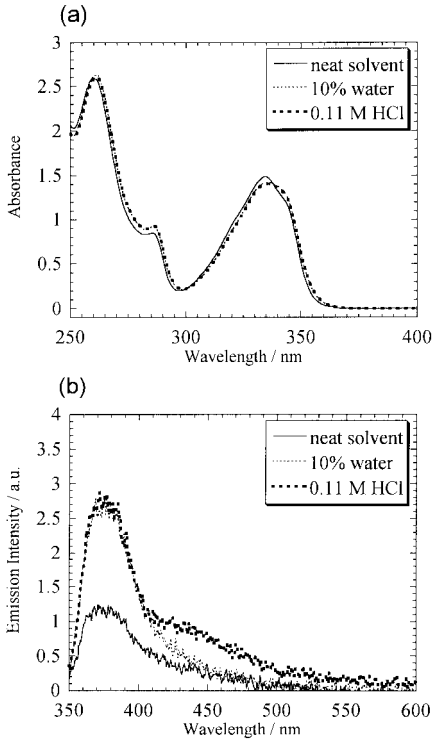

Figure 1. Effect of the addition of water and hydrochloric acid on (a) absorption and (b) emission spectra of xanthone in 2-propanol. The concentration of xanthone was kept at 2.0×10^{-4} M. The excitation wavelength used for recording the emission spectra was 308 nm.

Emission spectra were measured with a conventional fluorescence spectrometer (Hitachi model 850 or Shimadzu RF-5000). In absorption and emission experiments, samples were prepared with 2.1×10^{-4} M of Xn in 2-propanol. The concentration of HCl ranged from 1.0×10^{-2} to 1.0 M, and the amount of water was kept at 10% (v/v).

Results and Discussion

I. Absorption, Emission, and Transient Absorption Measurements. Absorption spectra of Xn taken under several conditions are shown in Figure 1a. The figure shows that addition of 10% (v/v) H_2O produces only a slight red shift and minor line broadening compared with the spectrum in neat 2-propanol. The broadening is probably caused by the coexistence of differently solvated Xn. An addition of 0.11 M HCl to the H_2O containing 2-propanol solution does not cause any change in the absorption spectrum. Therefore, it can be concluded that the ground state of Xn is not affected by the addition of a small amount of HCl.

Fluorescence spectra of Xn taken under different conditions are shown in Figure 1b. Figure 1b shows that the fluorescence intensity is enhanced considerably by the addition of 10% H_2O. By contrast, the addition of 0.11 M HCl does not change the fluorescence significantly except for the appearance of a weak shoulder around 450 nm. With the addition of increasing amounts of HCl, the relative intensity of the 450 nm band increases. The observations indicate that the excited singlet state of Xn is not affected by the addition of a small amount of HCl although in the presence of a large amount of HCl (>0.1 M) an exciplex of Xn with HCl may be formed. This is in accord

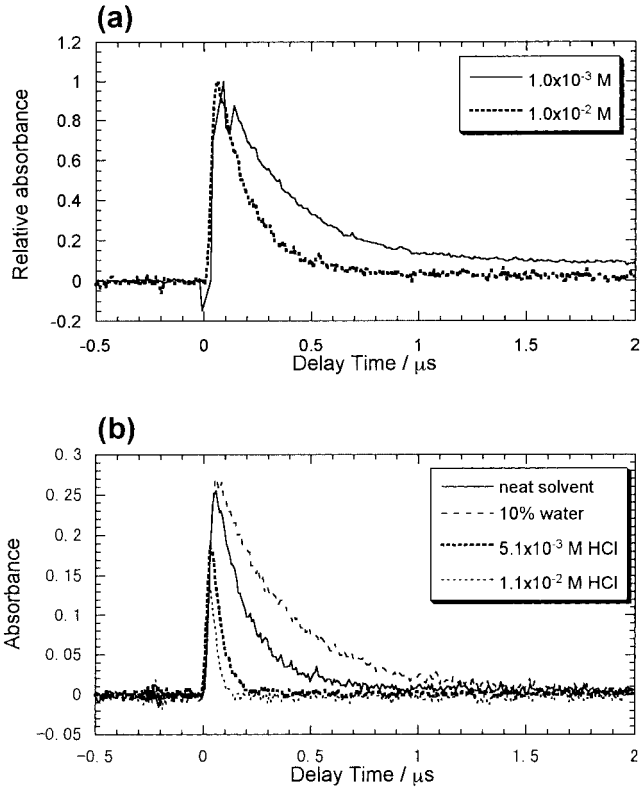

Figure 2. Decay of the transient absorption at 615 nm observed upon photoexcitation of xanthone in 2-propanol: (a) xanthone concentration dependence of the decay; (b) effect of addition of 10% water and hydrochloric acid.

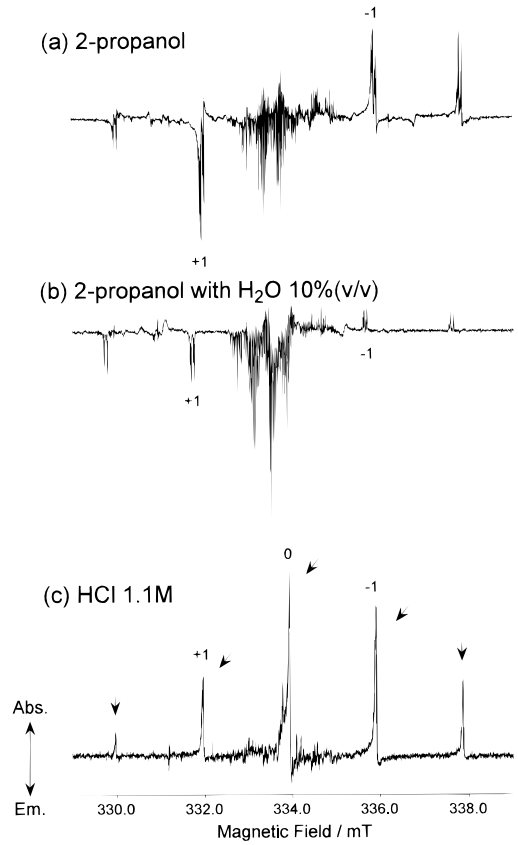

Figure 3. FT-EPR spectra of free radicals formed by photolysis of xanthone (1.0×10^{-2} M) observed for a delay time of 60 ns after the laser pulse: (a) in neat 2-propanol, (b) in 2-propanol with 10% (v/v) water, and (c) in 2-propanol with 10% (v/v) water and 1.1 M HCl. The arrows mark the resonance peaks due to 2HP.

with what is known about the singlet excited state of Xn. It has been reported that the isc rate from the $^1n\pi^*$ state of Xn in methanol is 2.3×10^{11} s^{-1}.[17] If the lifetime of ^{1}Xn* is on the order of 10 ps, the rate of excimer formation at an HCl concentration of 0.1 M should be too slow to compete with the decay of singlet excited Xn.

Transient absorption experiments were carried out to examine the characteristics of ^{3}Xn*. The absorption spectrum of ^{3}Xn* is known to have a maximum around 615 nm.[17] Figure 2a shows the decay curves of the transient absorption at 615 nm following the photolysis of Xn (10^{-2} and 10^{-3} M) in neat 2-propanol. The curves show an initial fast exponential decay followed by a long-lived component. The long-lived component is attributed to light absorption by the radicals (XnH) produced by H abstraction from solvent molecules. The fast component is ascribed to ^{3}Xn* decay and gives a rate constant of 3.2×10^6 s^{-1} for Xn (10^{-3} M) in neat 2-propanol. The rate of triplet decay for 10^{-3} M Xn (10^{-3} M) in 2-propanol containing 10% H_2O (cf. Figure 2b) is found to be 1.2×10^6 s^{-1}. These decay rates are considered to represent the rate constants (k_{HA}) for the hydrogen abstraction reaction of ^{3}Xn* with 2-propanol

$$^3\text{Xn}^* + \text{PrOH} \xrightarrow{k_{HA}} {}^\bullet\text{XnH} + {}^\bullet\text{PrOH} \qquad \text{(I)}$$

and establish that the hydrogen abstraction reaction is slowed in a solution containing H_2O. Triplet properties of Xn, including k_{HA}, are expected to depend on the structure of the solvation shell around ^{3}Xn*. Solvation by H_2O lowers the $^3\pi\pi^*$ state relative to the $^3n\pi^*$ state, thereby reducing the hydrogen abstraction rate.

Figure 2a shows that the lifetime of ^{3}Xn* is dependent on the Xn concentration. At 10^{-2} M Xn the decay rates are 6.0×10^6 s^{-1} in 2-propanol and 3.0×10^6 s^{-1} in the H_2O-containing solution. The concentration dependence is presumably due to the T−T annihilation process which increases in relative importance with increasing concentration of ^{3}Xn*.[33]

Contrary to what is found for the fluorescence, the transient absorption due to ^{3}Xn* is strongly quenched by the addition of small amounts of HCl as is shown in Figure 2b. At a concentration of 0.11 M HCl in a 2-propanol solution containing 10% H_2O, the transient absorption of ^{3}Xn* is completely quenched. A very drastic shortening of the triplet lifetime is already seen by the addition of 5×10^{-3} M HCl. From the HCl concentration dependence of the decay, the quenching rate constant is estimated to be 2.7×10^9 M^{-1} s^{-1}. This means that ^{3}Xn* is quenched by HCl with a near diffusion-controlled rate. It is important to note, however, that quenching by HCl does not enhance the long-lived absorption attributed to the XnH radical. Therefore, it can be concluded that the quenching of ^{3}Xn* by HCl is mainly due to a nonreactive process.

II. FT-EPR Measurements. *(1) Xn in Neat 2-Propanol and 2-Methyl-1-propanol.* The FT-EPR spectrum of radicals generated by laser excitation (308 nm) of Xn in neat 2-propanol is shown in Figure 3a. The sharp and strong lines at the low and high field sides of the spectrum are due to the 2HP radical, and the multiline signal in the center of the spectrum is assigned to the xanthone ketyl (XnH) radical[24] consistent with reaction scheme I. The spectrum shows an E*/A polarization pattern that can be accounted for in terms of a dominant E/A contribution generated by the ST_0 RPM and a minor net E component that may be due to TM CIDEP. That the triplet mechanism (TM) can give rise to an emissive signal contribution can be deduced from CW TREPR measurements of Xn triplets

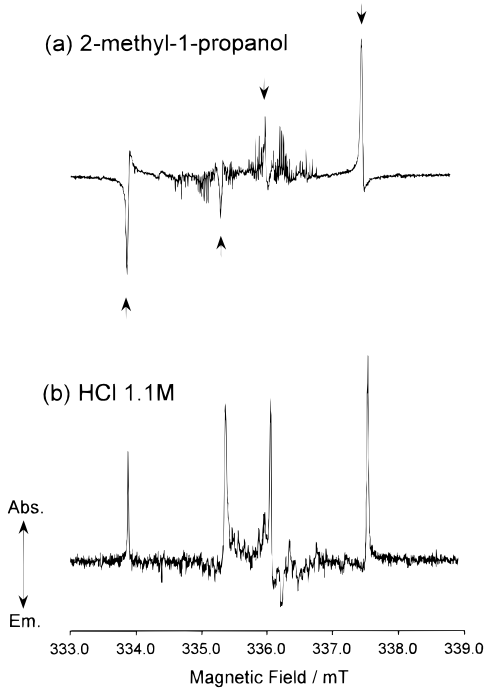

Figure 4. FT-EPR spectra of free radicals formed by photolysis of xanthone (1.0×10^{-2} M) observed for a delay time of 60 ns after the laser pulse: (a) in neat 2-methyl-1-propanol; (b) in 2-methyl-1-propanol with 1.1 M HCl. The arrows mark the resonance peaks due to 2MP.

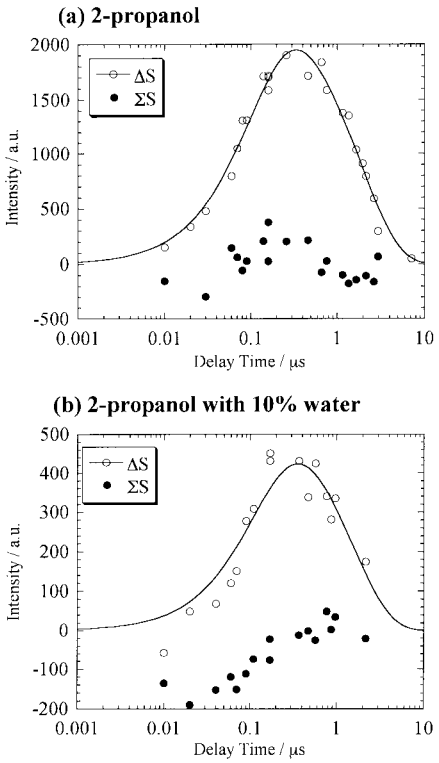

Figure 5. Time development of the EPR lines of the 2HP radical (a) in neat 2-propanol and (b) in 2-propanol with 10% water. ΣS shows the sum of the intensities of the $M_I = \pm 1$ hyperfine lines, and ΔS shows the difference of the intensities of the $+1$ and -1 lines.

in frozen solution.[10−12] It is also evident from the fact that CW EPR[29] and FT-EPR spectra of XnH and phenoxyl radicals formed by the hydrogen abstraction reaction of ^{3}Xn* with phenols show strong E polarization. The hydrogen abstraction reaction giving the XnH and phenoxyl radicals is known to be fast[37] so that the radicals can capture the spin polarization of precursor triplets. It should be noted, however, that in the Xn−propanol system the overall hydrogen abstraction rate ($\sim 3 \times 10^6$ s^{-1}, vide supra) is much too low for the TM to be effective given the fact that the triplet spin−lattice relaxation rate is expected to be $\sim 10^9$ s^{-1}. However, the character of ^{3}Xn* is known to be very sensitive to solvation structure as is evident from the observation of dual phosphorescence. It is quite possible, therefore, that ^{3}Xn* molecules with different solvation spheres have different hydrogen abstraction rates. If a small fraction of triplet Xn has a reaction rate approaching the triplet spin-relaxation rate, this can account for the small net E component observed. Alternatively, the radical triplet pair mechanism (RTPM) can be the source of E polarization.[28,29] Transient absorption measurements show that ^{3}Xn* is relatively long-lived, creating conditions where the RTPM mechanism can give rise to strong emissive polarization.[33−36] In fact, our CW TREPR experiments show that the relative intensity of the net emissive component is stronger at higher concentrations of Xn. This is consistent with what is expected for the RTPM.[33]

The polarization pattern shown in Figure 3a differs from the E/A* pattern previously found in a CW TREPR study of free radicals formed by the photolysis with 337 nm laser excitation of Xn in alcohols.[29] Moreover, as shown in Figure 4a, with 2-methyl-1-propanol as solvent, the FT-EPR spectrum shows an almost symmetrical E/A pattern, whereas in previous TREPR work an E/A* type spectrum was observed. To confirm these results, additional CW TREPR measurements were carried out in 2-propanol and 2-methyl-1-propanol at several temperatures and for delay times ranging from 0.5 to 2.0 μs. It was found that all CW TREPR spectra obtained by using the XeCl excimer laser (308 nm) as excitation source are of E*/A character, in agreement with the FT-EPR results. However, the spectra generated by using the third harmonic of a Nd:YAG laser (355 nm) are of E/A* type, in agreement with the results reported by Koga et al.[29] The results show that the CIDEP patterns in spectra of free radicals produced by photolysis of Xn in alcohols depend on the excitation wavelength. Assuming that net polarization is due to the TM, the wavelength dependence suggests that the spin selectivity of the singlet−triplet isc process is a function of the vibronic state reached with laser excitation. This could be the case if the isc rate is comparable to rates of vibrational deactivation and/or internal conversion within the singlet excited-state manifold, a condition that may be fulfilled in this case.[17] Further work is required to ascertain the mechanism giving rise to this intriguing phenomenon.

The time evolution of the EPR lines of the 2HP radical is shown in Figure 5. Depicted are the time developments of the net emissive component (ΣS, sum of the intensities of the $M_I = \pm 1$ hyperfine lines) and the RPM (E/A) signal contribution (ΔS, difference of the intensities of the $+1$ and -1 lines).[20] If the lifetime of the radical is long compared with the spin-relaxation time, the time evolution of the RPM spin polarization is represented by the following equation[31]

$$P_{\mathrm{RPM}} = P^0_{\mathrm{RPM}}\{\exp(-t/T_1^{\mathrm{R}}) - \exp(-k_{\mathrm{f}}t)\} + P^{\infty}_{\mathrm{RPM}}\{1 - \exp(-t/T_1^{\mathrm{R}})\} \quad (1)$$

Here, P^0_{RPM} and $P^{\infty}_{\mathrm{RPM}}$ are the initial polarization generated by the geminate RPM and the polarization at thermal equilibrium, respectively. T_1^{R} is the spin−lattice relaxation time of the 2HP radical, and k_{f} is the rate of RPM signal growth. In deriving eq 1, F-pair polarization created by radical termination reactions was ignored, and it was assumed that $k_{\mathrm{f}} \gg 1/T_1^{\mathrm{R}}$. When the hydrogen abstraction rate constant, k_{HA}, is less than the inverse

TABLE 1: Rate Constants of Formation and Decay of FT-EPR Signals of the 2HP Radical

	$k_f(\sum S)/s^{-1}$	$k_f(\Delta S)/s^{-1}$	$1/T_1^R/s^{-1}$
2-propanol		9.0×10^6	0.53×10^6
2-propanol with 10% H_2O		7.6×10^6	0.65×10^6
and HCl 1.2×10^{-2} M		14×10^6	0.63×10^6
and HCl 6.0×10^{-2} M	34×10^6	24×10^6	0.71×10^6
and HCl 1.2×10^{-1} M	29×10^6	20×10^6	0.66×10^6
and HCl 1.1 M	37×10^6	(37×10^6)	0.57×10^6
DBP in 2-propanol	32×10^6 [a]		(0.54×10^6)[a]
2-methyl-1-propanol		5.7×10^6	0.55×10^6
and HCl 1.1 M	22×10^6	17×10^6	0.56×10^6

[a] Rate constants for the 2,6-di-*tert*-butylphenoxyl radical. See text for details on the data analysis.

of the spectrometer response time and there is no quenching process of the triplet state other than the reaction, we should obtain $k_{HA} = k_f$. However, if the triplet concentration is relatively high, quenching due to T−T annihilation can be significant as shown by the transient absorption measurements (cf. Figure 2a), and in that case $k_{HA} < k_f$. The measured time developments of the signals are well simulated by eq 1 as shown for the 2-propanol solution by the solid line in Figure 5a. The rise and decay rates given by least-squares fits of the data to eq 1 give $k_f = 9.0 \times 10^6\ s^{-1}$, $1/T_1^R = 0.53 \times 10^6\ s^{-1}$ in 2-propanol and $k_f = 5.7 \times 10^6\ s^{-1}$, $1/T_1^R = 0.55 \times 10^6\ s^{-1}$ in 2-methyl-1-propanol. $k_f = 9 \times 10^6\ s^{-1}$ is larger than the hydrogen abstraction rate constant ($3.2 \times 10^6\ s^{-1}$ for 10^{-3} M Xn in 2-propanol) determined with the transient absorption technique. This is probably due to the effect of the T−T annihilation process, since the excitation laser power is stronger and the concentration of Xn is higher than that used in the transient absorption measurements. Signal decay rates agree quite well with previously reported values of the spin−lattice relaxation rate of the 2HP radical.[30,38]

(2) Effect of Addition of H_2O. Addition of H_2O to a solution of Xn in 2-propanol causes a decrease in signal intensity and a slight change in the CIDEP pattern (cf. Figure 3b). The spectrum shows a more pronounced E*/A character compared to that found in the absence of water (cf. Figure 3a), and the intensity of the hyperfine lines due to the XnH radical compared with those of the 2HP radical is greatly enhanced. Figure 5b shows that the E/A (ΔS) contribution to the 2HP spectrum develops more slowly than in pure 2-propanol, reflecting a slower hydrogen abstraction rate. Data derived from a least-squares fit using eq 1 are presented in Table 1. The (small) net E component ($\sum S$, Figure 5b) has an instrument-controlled rise time consistent with a TM contribution. The net E component of the integrated intensity of the XnH spectrum also rises quickly (cf. Figures 6a and 7a). From the decay of the emissive signal of XnH it is estimated that the spin−lattice relaxation time is $\sim 10\ \mu s$.

(3) Effect of Addition of HCl. Addition of HCl to the solutions of Xn in alcohols with 10% H_2O causes drastic changes in the CIDEP pattern. FT-EPR spectra of 0.01 M Xn in the presence of 1.1 M HCl in 2-propanol (10% H_2O) and 2-methyl-1-propanol (10% H_2O) are shown in Figures 3c and 4b, respectively. Both spectra show an overall A character with minor E/A component. Apparently, in these systems there is a CIDEP mechanism that makes a dominating net absorptive signal contribution and a small signal component stemming from the RPM. The results are in agreement with CW TREPR results reported previously.[29]

To obtain more detailed information, the HCl concentration dependence of the FT-EPR spectra was investigated. The FT-EPR spectra obtained at several HCl concentrations with a delay

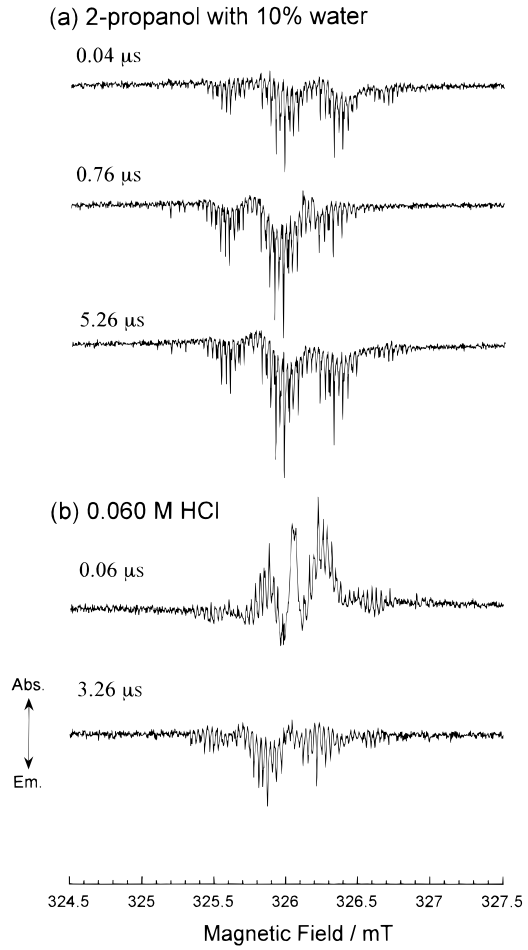

Figure 6. Time evolution of the FT-EPR spectra of the xanthone ketyl radical (a) in 2-propanol with 10% water and (b) in 2-propanol with 10% water and 0.060 M HCl.

time of 60 ns are shown in Figure 8. It is seen that the contribution of the net A polarization increases with an increase in HCl concentration. At 0.01 M HCl the spectrum still has a dominant E/A polarization component, but the overall signal intensity is reduced considerably. The change in polarization to net absorption occurs at low HCl concentration, and the spectrum is already completely absorptive for [HCl] = 0.06 M (cf. Figure 8b). Further increases in HCl concentration leave the polarization pattern and signal intensity virtually unchanged.

The time developments of the net absorptive signal contribution ($\sum S$) and RPM signal contribution (ΔS) to the spectrum of 2HP at four HCl concentrations are shown in Figure 9. In Figure 9a the lines depict least-squares fits of the ΔS data points to eq 1, and in Figure 9b the lines represent the fits of the $\sum S$ points to the equation for the time development of TM polarization,[31]

$$P_{TM} = P^0_{TM}\{\exp(-t/T_1^R) - \exp[-(k_{HA} + 1/T_1^T)t]\} + P^\infty_{TM}\{1 - \exp(-t/T_1^R)\} \quad (2)$$

Here, P^0_{TM} and P^∞_{TM} are the initial polarization and the thermal equilibrium polarization, respectively. T_1^T is the spin−lattice relaxation time of the triplet state, k_{HA} is the rate constant of the hydrogen abstraction reaction, and it is assumed that $(k_{HA} + 1/T_1^T) \gg 1/T_1^R$. It is found that $(k_{HA} + 1/T_1^T)$ is larger than the inverse of the instrument response time, so that the rate of net A signal growth is $\sim 3 \times 10^7\ s^{-1}$. Table 1 gives the rate constants of signal growth and decay derived from the experimental data.

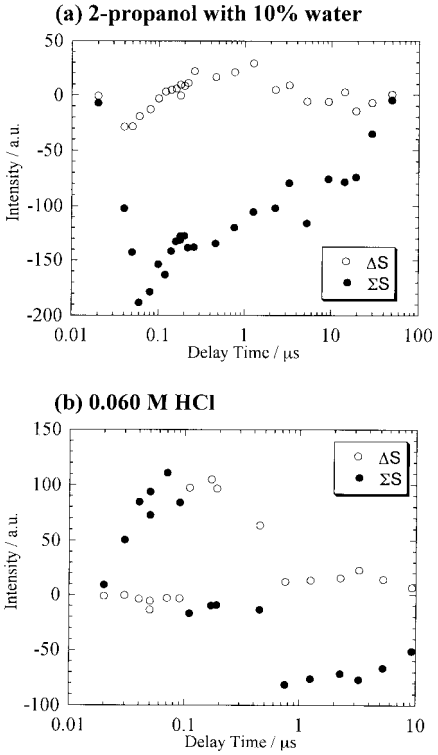

Figure 7. Time development of the EPR lines of the xanthone ketyl (XnH) radical in 2-propanol (a) with 10% water and (b) with 10% water and 0.060 M HCl. ΣS shows the sum of the integrated intensities of high field and low field lines and ΔS the difference between high and low field lines.

According to transient optical absorption measurements, the rate constant of (mainly nonreactive) triplet quenching by HCl is $\sim 2.7 \times 10^9$ M^{-1} s^{-1}. The quenching rate at 0.1 M HCl (2.7×10^8 s^{-1}), therefore, is already some 2 orders of magnitude higher than the hydrogen abstraction rate in neat 2-propanol and 2-propanol with 10% H_2O. Even so, reasonably strong EPR signals are recorded in the presence of HCl up to a concentration as high as 1 M. It must be concluded that HCl addition not only introduces a path of efficient nonreactive triplet decay but also increases the rate of free radical formation. That EPR signals remain strong even though the nonreactive triplet decay route dominates may in part be due to the fact that the reaction rate is high enough for the radicals to capture spin polarization of precursor triplets.[32]

In the presence of HCl, CIDEP spectra of the XnH radical also show absorptive polarization as shown in Figures 6b and 8b. This is consistent with the assignment of the net polarization to TM CIDEP. The signal intensity of the XnH spectrum relative to that of the 2HP radical diminishes noticeably as the concentration of HCl increases. This may be due to line broadening caused by proton exchange. The effect of proton exchange is also evident in the spectrum of 2HP; a comparison of the spectra given in Figure 3 shows that addition of HCl leads to a loss of the second order hyperfine structure that is clearly evident in the spectra from 2HP in 2-propanol (with and without H_2O).

Figures 6b and 7b show that, in a 2-propanol solution containing 0.06 M HCl, the XnH spectrum shows a polarization inversion from absorptive to emissive with increasing time. The emissive polarization cannot arise from the RTPM because ^{3}Xn* is already completely quenched by HCl in less than 0.1 μs according to the transient absorption data. At this point the cause of this polarization inversion is not understood.

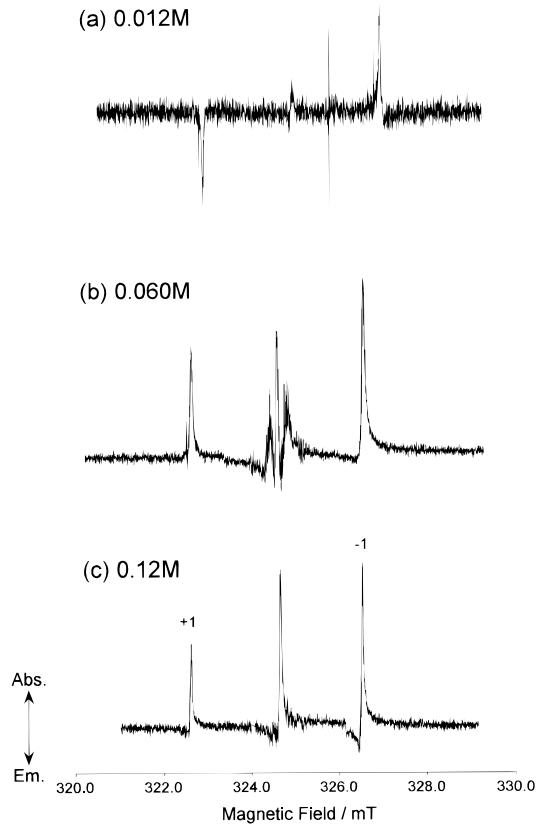

Figure 8. HCl concentration dependence of the FT-EPR spectra of free radicals generated by the photoreduction of xanthone in 2-propanol with 10% H_2O. The HCl concentrations are (a) 0.012 M, (b) 0.060 M, and (c) 0.12 M. The concentration of xanthone was kept at 0.010 M.

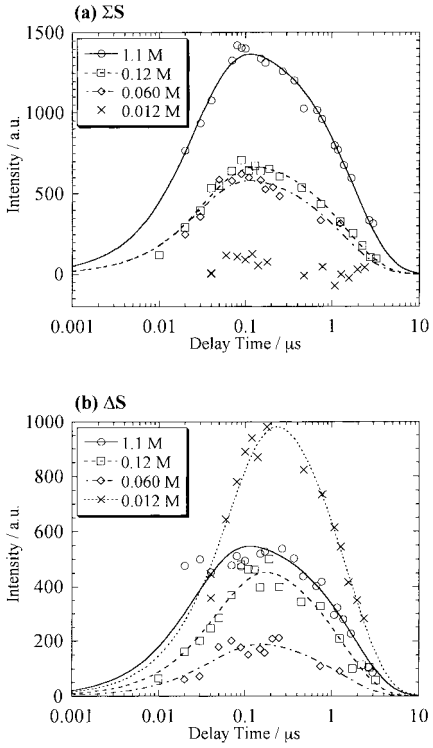

Figure 9. Time developments of the sum of the integrated intensities of high field and low field lines (ΣS) and the difference in intensities of the high and low field lines (ΔS) in the spectrum of the 2HP radical for various HCl concentrations.

III. Reaction and CIDEP Mechanisms Generating A Polarization. At the HCl concentration required to produce a

complete change in the spin polarization pattern ([HCl] < 0.1 M), the optical absorption spectrum of Xn shows no change from that observed in 2-propanol with 10% H_2O. Also, the fluorescence spectrum remains virtually unaffected in this HCl concentration range. These findings argue against ground-state complex formation as the cause of the polarization change. The short singlet excited-state lifetime[17] also rules out the possibility of singlet exciplex formation. By contrast, the change in CIDEP occurs over a concentration range where the lifetime of ^{3}Xn* is strongly affected as well. This suggests that triplet quenching by HCl is the source of the A polarization found in the EPR spectra. It has been found that addition of H_2SO_4, HNO_3, or LiCl to solutions of Xn in alcohols does not affect the spin polarization.[29] Apparently, the presence of both H^+ and Cl^- is required to produce overall A polarization.

The following mechanism is proposed for the effect of HCl on triplet lifetime, hydrogen abstraction rate, and spin polarization:

$$^3\mathrm{Xn}^* + \mathrm{H}^+ \rightleftarrows {}^3\mathrm{XnH}^{+}* \qquad \text{(II)}$$

$$^3[\mathrm{XnH}^+]^* + \mathrm{Cl}^- \rightleftarrows {}^3[\mathrm{XnHCl}]^* \qquad \text{(III)}$$

$$^3[\mathrm{XnHCl}]^* \rightarrow\!\!\rightarrow \mathrm{Xn} + \mathrm{H}^+ + \mathrm{Cl}^- \qquad \text{(IV)}$$

$$^3[\mathrm{XnHCl}]^* + \mathrm{HROH} \rightarrow \mathrm{XnH}^{\bullet} + {}^{\bullet}\mathrm{ROH} + \mathrm{H}^+ + \mathrm{Cl}^- \qquad \text{(V)}$$

It is expected that, at low concentration in 2-propanol with 10% H_2O, HCl is dissociated so that it is assumed that the dominant triplet quenching path (IV) is preceded by a two-step triplet exciplex formation process ((II) and (III)). Reaction V competes with the nonreactive quenching process, but the quantum yield of the hydrogen abstraction reaction is relatively low. The exciplex may have charge-transfer character (^{3}[XnH$^{\bullet}\cdots$Cl$^{\bullet}$]), and since the chlorine radical is quickly quenched by alcohols,[39] this can account for the strong increase in hydrogen abstraction rate.

The net A polarization in the free radicals can have its origin in the nonreactive quenching of the triplet state. Step IV involves a triplet−singlet isc process that is expected to be highly sublevel dependent. If quenching from the upper spin sublevel is faster than quenching from the lower levels, then the reaction involving ^{3}[XnHCl]*, if competitive with spin−lattice relaxation, will produce radicals with absorptive spin polarization. It is noted that this mechanism is similar to the recently proposed spin−orbit coupling-induced polarization mechanism in the electron transfer between xanthene dyes and *p*-quinones studied by Tero-Kubota's group.[40,41]

Koga et al.[29] propose that the effect of HCl addition on the CIDEP spectra of the radicals produced by the photolysis of Xn in alcohols could be due to ground-state complexation between Xn and HCl. The spin selectivity of isc from the excited singlet state of [XnHCl] could produce excess population in the −1 spin state of ^{3}[XnHCl]* which could give rise to absorptive TM CIDEP. The fact that the optical absorption spectrum of Xn shows no evidence of complex formation argues against this interpretation. The mechanism also does not account for the dynamic quenching of triplet Xn by HCl observed in the present study.

Acknowledgment. Prof. Hisao Murai in Tohoku University is thanked for useful discussions. This work was supported by Scientific Research Grant-in-Aid for International Scientific Research (No. 08044071) provided by the Ministry of Education Science and Culture of Japan. K.O. was partially supported by Research Fellowships of the Japan Society for the Promotion of Science for Young Scientists. H.v.W. wishes to thank the members of the Chemistry Department of Kyoto University for their hospitality and acknowledges financial support from the Division of Chemical Sciences, Office of Basic Energy Sciences of the US Department of Energy (DE-FG02-84ER-13242).

References and Notes

(1) Yang, N. C.; Murov, S. L. *J. Chem. Phys.* **1966**, *45*, 4358.
(2) Pownall, H. J.; Huber, J. R. *J. Am. Chem. Soc.* **1971**, *93*, 6429.
(3) Long, M. E.; Lim, E. C. *Chem. Phys. Lett.* **1973**, *20*, 413.
(4) Chakrabarti, A.; Hirota, N. *J. Phys. Chem.* **1976**, *80*, 2966.
(5) Pownall, H. J.; Mantulin, W. M. *Mol. Phys.* **1976**, *31*, 1393.
(6) Connors, R. E.; Walsh, P. S. *Chem. Phys. Lett.* **1977**, *52*, 436.
(7) Scaiano, J. C. *J. Am. Chem. Soc.* **1980**, *102*, 7747.
(8) Vala, M.; Hurst, J.; Trabjerg, I. *Mol. Phys.* **1981**, *43*, 1219.
(9) Griesser, H. J.; Bramley, R. *Chem. Phys.* **1982**, *67*, 361, 373.
(10) Sakaguchi, Y.; Hayashi, H.; Murai, H.; I'Haya, Y. J.; Mochida, K. *Chem. Phys. Lett.* **1985**, *120*, 401.
(11) Sakaguchi, Y.; Hayashi, H.; Murai, H.; I'Haya, Y. *J. Am. Chem. Soc.* **1988**, *110*, 7479.
(12) Murai, H.; Minami, M.; I'Haya, Y. J. *J. Phys. Chem.* **1988**, *92*, 2120.
(13) Koyanagi, M.; Terada, T.; Nakashima, N. *J. Chem. Phys.* **1988**, *89*, 7349.
(14) Ohara, K.; Murai, H. *Bull. Chem. Soc. Jpn.* **1989**, *62*, 2435.
(15) Baba, M.; Kamei, T.; Kiritani, M.; Yamauchi, S.; Hirota, N. *Chem. Phys. Lett.* **1991**, *185*, 354.
(16) Murai, H.; Kuwata, K. *J. Phys. Chem.* **1991**, *95*, 6247.
(17) Cavaleri, J. J.; Prater, K.; Bowman, R. M. *Chem. Phys. Lett.* **1996**, *259*, 495.
(18) McLauchlan, K. A.; Hore, J. H. *Advanced EPR: Application in Biology and Biochemistry*; Hoff, A. J., Ed.; Elsevier: Amsterdam, 1989.
(19) McLauchlan, K. A. In *Modern Pulsed and Continuous-Wave Electron Spin Resonance*; Kevan, L., Bowman, M. K., Eds.; John Wiley & Sons: New York, 1990; Chapter 7.
(20) van Willigen, H.; Levstein, P. R.; Ebersole, M. H. *Chem. Rev.* **1993**, *93*, 173.
(21) Adrian, F. J. *J. Chem. Phys.* **1971**, *54*, 3918; **1972**, *57*, 5107.
(22) Pedersen, J. B.; Freed, J. H. *J. Chem. Phys.* **1973**, *58*, 2746; **1973**, *59*, 2869.
(23) Atkins, P. W.; Evans, G. T. *Mol. Phys.* **1974**, *27*, 1633.
(24) Pedersen, J. B.; Freed, J. H. *J. Chem. Phys.* **1975**, *62*, 1706.
(25) Buckley, C. D.; Hunter, D. A.; Hore, P. J.; McLauchlan, K. A. *Chem. Phys. Lett.* **1987**, *86*, 137.
(26) Closs, G. L.; Forbes, M. D. E. *J. Phys. Chem.* **1987**, *91*, 3592.
(27) Blättler, C.; Jent, F.; Paul, H. *Chem. Phys. Lett.* **1990**, *166*, 375.
(28) Kawai, A.; Okutsu, T.; Obi, K. *J. Phys. Chem.* **1991**, *95*, 9130.
(29) Koga, T.; Ohara, K.; Kuwata, K.; Murai, H. *J. Phys. Chem. A*, in press.
(30) Levstein, P. R.; van Willigen, H. *J. Chem. Phys.* **1991**, *95*, 900.
(31) Ohara, K.; Hirota, N.; Steren, C. A.; van Willigen, H. *Chem. Phys. Lett.* **1995**, *232*, 169.
(32) Yamauchi, S.; Hirota, N. *J. Phys. Chem.* **1984**, *88*, 4631.
(33) Ohara, K.; Hirota, N. *Bull. Chem. Soc. Jpn.* **1996**, *69*, 1517.
(34) Blättler, C.; Jent, F.; Paul, H. *Res. Chem. Intermed.* **1991**, *16*, 201.
(35) Kawai, A.; Obi, K. *J. Phys. Chem.* **1992**, *96*, 5701.
(36) Michaeli, S.; Meiklyar, V.; Schulz, M.; Möbius, K.; Levanon, H. *J. Phys. Chem.* **1994**, *98*, 7444.
(37) Ishiwata, N.; Murai, H.; Kuwata, K. *Res. Chem. Intermed.* **1993**, *19*, 59.
(38) Tominaga, K.; Yamauchi, S.; Hirota, N. *J. Chem. Phys.* **1990**, *92*, 5175.
(39) Kawai, A.; Okutsu, T.; Obi, K. *Chem. Phys. Lett.* **1990**, *174*, 213.
(40) Katsuki, K.; Akiyama, K.; Ikegami, Y.; Tero-Kubota, S. *J. Am. Chem. Soc.* **1994**, *116*, 12065.
(41) Katsuki, K.; Akiyama, K.; Tero-Kubota, S. *Bull. Chem. Soc. Jpn.* **1995**, *68*, 3383.
(42) Murai, H.; Minami, M.; I'Haya, Y. J. *J. Chem. Phys.* **1994**, *101*, 4514.